

Article

Optimal Auxiliary Functions Method for a Pendulum Wrapping on Two Cylinders

Vasile Marinca¹ and Nicolae Herisanu^{1,2,*}

¹ Center for Fundamental Technical Research, Romanian Academy, 300222 Timisoara, Romania; vmarinca@mec.upt.ro

² Faculty of Mechanics, University Politehnica Timisoara, 300222 Timisoara, Romania

* Correspondence: nicolae.herisanu@upt.ro

Received: 21 July 2020; Accepted: 11 August 2020; Published: 14 August 2020



Abstract: In the present work, the nonlinear oscillations of a pendulum wrapping on two cylinders is studied by means of a new analytical technique, namely the Optimal Auxiliary Functions Method (OAFM). The equation of motion is derived from the Lagrange's equation. Analytical solutions and natural frequency of the system are calculated. Our results obtained through this new procedure are compared with numerical ones and a very good agreement was found, which proves the accuracy of the method. The presented numerical examples show that the proposed approach is simple, easy to implement and very accurate.

Keywords: simple pendulum; optimal auxiliary functions method

1. Introduction

The study of the simple pendulum has a long history. During the Renaissance, Leonardo da Vinci made some drawings related to the motion of pendulum, without realizing at that time its great importance for timekeeping. Beginning around 1602, Galileo Galilei studied for the first time the properties of pendulum, isochronisms, and found that the period of this system is approximately independent of the amplitude or with the swing. Additionally, he demonstrated that the period is proportional to the square root of the length of the pendulum, but independent on the mass. Forty years later he conceived and dictated to his son a design for a pendulum clock. The pendulum was the first harmonic oscillator used by human being [1]. In 1673, Huygens discovered that the period of the pendulum is identical, no matter if it hung from its centre of oscillation or from its pivot [2]. In 1818 Henry Kater invented the so-named reversible Kater's pendulum, making very accurate measurements of gravity possible. In 1851 Foucault made his investigations known, and a "pendulum mania" broke out [3]. Around 1900, the need for higher precision clocks led to the use of low-thermal-expansion materials for pendulum rods. In 1921, the quartz crystal oscillator was invented, and in 1927 quartz clocks replaced pendulum clocks [4]. Pendulum gravimeters were replaced by "free fall" gravimeters in the 1950s [5], but pendulum instruments continued to be considered into the 1970s. In 1721, G. Graham [6] invented the mercury pendulum, whose weight is represented by a container of mercury, in which case the pendulum rod gets longer with rising temperature. In 1726, J. Harrison invented the gridiron pendulum, consisting of alternating rods made of different metals, with totally different thermal expansion properties (steel and zinc or brass, respectively). In 1896, C.E. Guillaume invented the nickel-steel alloy [4]. The invar pendulum was used for the first time in the Riefler regulator clock, achieving an excellent accuracy. In 1826 G. Airy proved the smallest disturbing effect of the drive force on the period if given as a short type of pendulum, such as the Repsold-Bessel pendulum [7], Van Sterneck and Mendelhall gravimeters, double pendulum gravimeters, Gulf gravimeter [8], and so on.

Dynamic mechanical systems possessing the pendulum arise in many domains of activity and many scientists paid attention to obtaining a governing equation of pendulums. The above-mentioned studies were later extended to other types of pendulum with different conditions along their dynamic behavior.

Hamouda and Pierce [9] analyzed the blades of a helicopter rotor (similar to a simple pendulum) to suppress the root reactions. The general nonlinear equations of motion are linearized. They consider the hingeless rotor blade excited by a harmonic variation of span wise air load distribution. Simple flap and lead-lag pendulum are treated individually. The pendulum mass effectiveness was also investigated.

A comprehensive discussion of the corrections needed to accurately measure the acceleration of gravity using a plane pendulum is provided by Nelson and Olson [10]. A simple laboratory experiment was described, in which g was determined to four significant figures of accuracy. The effect of the Coriolis force acting on the bob during station is evaluated, adapting a spring-pendulum system analysis to the nearly stiff limit. In their study, the linear and quadratic damped were used and perturbation expansion of the small dimensionless parameter was developed.

Ge and Ku [11] extended the Melnikov approach (which is traditionally restricted to study in weak non-linear phenomena including sufficient small harmonic excitation) to a pendulum suspended on a rotating arm described by two-dimensional differential equations. These equations possess strongly odd nonlinear function of the displacement and are subjected to large harmonic excitation.

Nester et al. [12] presented an experimental investigation into the dynamic response of rotor systems fitted with centrifugal pendulum vibration absorbers. Two types of absorbers are considered, which exhibit different types of nonlinear behavior.

The spatial double pendulum, comprising two pendulums that swing in different planes is analyzed in [13] by Bendersky and Sandler. Some Matlab codes were proposed to solve the nonlinear differential equations. The frequency spectra were obtained using Fourier transformation. Solutions of free vibrations and frequency spectra were employed in dynamic investigations for different initial conditions of motion.

A small ellipticity of the driving, perturbing the classical parametric pendulum, was studied by Horton et al. [14]. Warminski and Kecik analyzed the motion of a nonlinear oscillator with attached pendulum, excited by the moment of its suspension point, the oscillator, and the pendulum being strongly coupled by inertial terms [15]. In [16], Kecik and Warminski proposed a new suspension composed of a semiactive magnetorheological damper and a nonlinear spring in order to control motions. In this way, unstable areas and the chaotic or rotating motion of the pendulum are reduced.

A variation of the simple pendulum involving square plates was investigated by Rafat et al. [17]. The equilibrium configurations and normal modes of oscillations are obtained. The equations of motion were solved numerically to produce Poincaré sections. The accurate analytic solution of the nonlinear pendulum differential equation is obtained using homotopy analysis technique by Turkyilmazoglu [18]. The obtained explicit analytical expressions for the frequency, period and displacement are compared with numerical ones.

Awrejcewicz [19] studied the mathematical pendulum motion oscillating in a plane rotating with angular velocity. The three-dimensional double pendulum, which is coupled by two universal joints, is investigated in [20]. The multiple scales method was used in [21] for recognizing resonances occurring in a parametrically and externally excited nonlinear spring pendulum. Energy balance method was employed in [22] to obtain approximations for achieving the nonlinear frequency for pendulum attached to rolling wheels that is restrained by a spring. The nonlinear oscillations of pendulum wrapping on two cylindrical bases were investigated by Mazaheri et al. [23]. To obtain an analytical solution, the multiple scale method is used and there are analyzed effects of amplitude and radius of cylinder.

Boubaker presented in [24] a survey on the inverted pendulum in nonlinear control theory offering an overall picture of historical, current and trend developments. Synchronization of two pendulums mounted on a mutual base is investigated by Alevras et al. [25] and the response of pendulum was obtained when the base was excited by a random sinusoidal force. The influence of an external

harmonic excitation on a chain of nonlinear pendulum was explored by Jallouli et al. in [26] in case of simultaneous external and parametric excitations.

In this paper we propose a novel procedure, the Optimal Auxiliary Functions Method (OAFM), to investigate the nonlinear oscillations of a simple pendulum bounded by two cylinders at the point of suspension. The length of this pendulum varies due to wrapping around the cylinders. Such systems of pendulum with such additional conditions along with their dynamic behavior could find applications in aerospace engineering and shipping engineering.

Unlike other solution procedures applied to find approximate analytical solutions to nonlinear dynamical systems, the proposed approach is based upon original construction of the solution using a moderate number of convergence-control parameters, which are basic components of the original auxiliary functions introduced in the present developments. These parameters lead to a high precision, comparing our approximate solutions with exact or numerical ones.

The accuracy of the obtained results is proved by numerical developments, which validate the analytical results.

2. The Optimal Auxiliary Functions Method

The basics of OAFM can be found in [27,28], where OAFM is applied to solve different problems. In order to develop an application of the OAFM, let us consider the nonlinear differential equation [27–29]:

$$L[u(x)] + g(x) + N[u(x)] = 0, \tag{1}$$

where L is the linear operator, N is the nonlinear operator, and g is a known function, x being an independent variable and $u(x)$ an unknown function at this stage. The initial or boundary conditions are:

$$B\left(u(x), \frac{du(x)}{dx}\right) = 0. \tag{2}$$

It is well-known that it is often very hard to find an exact solution for strongly nonlinear equations of type (1) and (2) [30]. In order to find the approximate solution $\tilde{u}(x)$, we suppose this can be expressed as

$$\tilde{u}(x, C_i) = u_0(x) + u_1(x, C_i), \quad i = 1, 2, \dots, s, \tag{3}$$

where the initial and the first approximation will be obtained, as described below. After the substitution of Equation (3) into Equation (1), one obtains

$$L[u_0(x)] + L[u_1(x, C_i)] + g(x) + N[u_0(x) + u_1(x, C_i)] = 0, \tag{4}$$

where $C_i, i = 1, 2, \dots, s$ are the convergence-control parameters, which will be rigorously determined.

The initial approximation $u_0(x)$ may be determined from the linear equation

$$L[u_0(x)] + g(x) = 0, \quad B\left(u_0(x), \frac{du_0(x)}{dx}\right) = 0. \tag{5}$$

while the first approximation is obtained from Equations (4) and (5):

$$L[u_1(x, C_i)] + N[u_0(x) + u_1(x, C_i)] = 0 \quad B\left(u_1(x, C_i), \frac{du_1(x, C_i)}{dx}\right) = 0. \tag{6}$$

The nonlinear term from Equation (6) is expanded as

$$N[u_0(x) + u_1(x, C_i)] = N[u_0(x)] + \sum_{k=1}^n \frac{u_1^k(x, C_i)}{k!} N^{(k)}[u_0(x)], \dots \tag{7}$$

In order to avoid the difficulties appearing in solving Equation (6) and also to accelerate the convergence of the solution $\tilde{u}(x, C_i)$, instead of the last term, one can suggest another expression, so that this equation may be rewritten as

$$L[u_1(x, C_i)] + A_1(u_0(x), C_j)F(N[u_0(x)]) + A_2(u_0(x), C_k) = 0$$

$$B\left(u_1(x, C_i), \frac{du_1(x, C_i)}{dx}\right) = 0, \quad i = 1, 2, \dots, s \tag{8}$$

where A_1 and A_2 are auxiliary functions which depend on initial approximation $u_0(x)$ and some convergence-control parameters C_j , and C_k , $j = 1, 2, \dots, p$, $k = p + 1, p + 2, \dots, s$, and $F(N[u_0(x)])$ are functions which depend on the expressions which appear within the nonlinear term $N[u_0(x)]$. It should be emphasized that the auxiliary functions A_1 and A_2 (namely optimal auxiliary functions) and $F(N[u_0(x)])$ are not unique, but these auxiliary functions are of the same form, similar to $u_0(x)$. More precisely, if $u_0(x)$ is a polynomial function, then A_1 and A_2 are sums of polynomial functions. If $u_0(x)$ is an exponential function, then A_1 and A_2 are sums of exponential functions. In the case of $u_0(x)$, which is a trigonometric function, it follows that A_1 and A_2 are sums of trigonometric functions, and so on.

In the case when $N[u_0(x)] = 0$, then $u_0(x)$ is the exact solution of the original equation.

The initially unknown convergence-control parameters C_j and C_k may be rigorously and optimally determined via various methods, among them being the least square method, Galerkin method, collocation method, Ritz method, but the preferred one should be minimizing the square residual error:

$$J(C_1, C_2, \dots, C_s) = \int_{(D)} R^2(x, C_j, C_k) d\tau, \quad j = 1, 2, \dots, p, \quad k = p + 1, p + 2, \dots, s, \tag{9}$$

where

$$R(x, C_j, C_k) = L[\tilde{u}(x, C_i)] + g(x) + N[\tilde{u}(x, C_i)], \quad j = 1, 2, \dots, p, \quad k = p + 1, p + 2, \dots, s, \quad i = 1, 2, \dots, s, \tag{10}$$

in which the approximate solution $\tilde{u}(x, C_i)$ is given by Equation (3). The unknown parameters C_1, C_2, \dots, C_s can be identified from the conditions

$$\frac{\partial J}{\partial C_1} = \frac{\partial J}{\partial C_2} = \dots = \frac{\partial J}{\partial C_s} = 0. \tag{11}$$

Similar results could be obtained by imposing the conditions

$$R(x_1, C_j) = R(x_2, C_j) = \dots = R(x_i, C_j) = 0, \quad x_i \in D, \quad i = 1, 2, \dots, s$$

By using this above presented approach, the approximate solution is completed after the determination of the optimal values of convergence-control parameters C_i , $i = 1, 2, \dots, s$. Hence, our procedure involves the auxiliary functions A_1 and A_2 which provide an effective way to adjust and control the convergence of the final solutions $\tilde{u}(x, C_i)$. It is necessary to remark the importance of carefully choosing the functions A_1 and A_2 involved in the construction of the first-order approximation $u_1(x, C_i)$. It was already proved that our method is easily applicable to solve nonlinear problems without small or large parameters, including systems with more degrees of freedom [27].

3. Equation of Motion

In what follows, we present the governing equation of the simple pendulum wrapping around two cylinders at the point of suspension [23]. The length of the pendulum is L while the radius of cylinders is r (Figure 1).

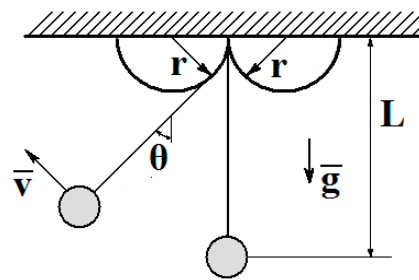


Figure 1. Simple pendulum wrapping around the cylinders.

The motion of the system is described by the generalized coordinate θ , but the string length is changing. The kinetic energy can be expressed in the form

$$T = \frac{1}{2}m(L - r|\theta|)^2\dot{\theta}^2, \tag{12}$$

where m is the mass of pendulum and the dot denotes differentiation with respect to time.

The potential energy becomes

$$U = mg[L - (L - r|\theta|) \cos \theta - r \sin \theta]. \tag{13}$$

From the Lagrange’s equation one can put

$$m(L - r|\theta|)^2\ddot{\theta} - 2mr(L - r|\theta|)(\text{sgn}\theta)\dot{\theta}^2 + mr(L - r|\theta|)\dot{\theta}(\text{sgn}\theta) + mg(L - r|\theta|) \sin \theta - mgr \cos \theta(\text{sgn}\theta) + mgr \cos \theta(\text{sgn}\theta) = 0 \tag{14}$$

After some manipulation, one obtains:

$$(L - r|\theta|)\ddot{\theta} + g \sin \theta - r\dot{\theta}^2(\text{sgn}\theta) = 0, \tag{15}$$

$$\ddot{\theta} - a\dot{\theta}|\dot{\theta}| + \frac{g}{L} \sin \theta - a\dot{\theta}^2(\text{sgn}\theta) = 0, \tag{16}$$

where $a = r/L$. The initial conditions for Equation (16) are

$$\theta(0) = A, \quad \dot{\theta}(0) = 0. \tag{17}$$

4. Application of OAFM to a Pendulum Wrapping on Two Cylinders

If one inserts the independent variable $\tau = \Omega t$ and the dependent variable $\varphi = \theta A^{-1}$, then the governing Equations (16) and (17) become

$$\varphi'' - aA\varphi''|\varphi| + \frac{g}{AL\Omega^2} \sin A\varphi - aA\varphi'^2(\text{sgn}\varphi) = 0, \tag{18}$$

$$\varphi(0) = 1, \quad \varphi'(0) = 0, \tag{19}$$

where Ω is the frequency of the system and prime denotes differentiation with respect to τ .

For Equation (18), the linear operator can be identified in the form

$$L[\varphi(\tau)] = (\varphi'' + \varphi), \tag{20}$$

with $g(\tau) = 0$, while the corresponding nonlinear operator is

$$N[\varphi(\tau, \Omega)] = -\varphi - aA\varphi''|\varphi| + \frac{g}{AL\Omega^2} \sin A\varphi - aA\varphi'^2(\text{sgn}\varphi). \tag{21}$$

The Equation (5) becomes

$$\varphi''_0 + \varphi_0 = 0, \quad \varphi_0(0) = 1, \varphi'_0(0) = 0, \tag{22}$$

and has the solution

$$\varphi_0(\tau) = \cos \tau. \tag{23}$$

Substituting Equation (23) into Equation (21), we obtain

$$N[\varphi_0(\tau, \Omega)] = -\cos \tau + aA \cos \tau |\cos \tau| + \frac{g}{AL\Omega^2} \sin(A \cos \tau) - aA \sin^2 \tau (\text{sgn}(\cos \tau)). \tag{24}$$

Having in view that

$$\cos \tau |\cos \tau| = \cos^2 \tau (\text{sgn}(\cos \tau)), \tag{25}$$

$$\cos^2 \tau (\text{sgn}(\cos \tau)) - \sin^2 \tau (\text{sgn}(\cos \tau)) = \cos 2\tau (\text{sgn}(\cos \tau)), \tag{26}$$

$$(\text{sgn}(\cos \tau)) = \frac{4}{\pi} \left(\cos \tau - \frac{1}{2} \cos 3\tau + \frac{1}{5} \cos 5\tau - \frac{1}{7} \cos 7\tau + \frac{1}{9} \cos 9\tau + \dots \right), \tag{27}$$

$$\begin{aligned} \sin(A \cos \tau) &= \left(A - \frac{A^3}{8} + \frac{A^5}{192} - \frac{A^7}{9216} + \frac{A^9}{737280} + \dots \right) \cos \tau \\ &+ \left(-\frac{A^3}{24} + \frac{A^5}{384} - \frac{A^7}{15360} + \frac{A^9}{1105920} - \dots \right) \cos 3\tau + \left(\frac{A^5}{1920} - \frac{A^7}{46080} \right. \\ &\left. + \frac{A^9}{2580480} + \dots \right) \cos 5\tau + \left(-\frac{A^7}{322560} + \frac{A^9}{10321920} + \dots \right) \cos 7\tau + \left(\frac{A^9}{92897280} + \dots \right) \cos 9\tau \end{aligned}, \tag{28}$$

and substituting Equations (25)–(28) into Equation (24), one can get

$$\begin{aligned} N[\varphi_0(\tau, \Omega)] &= \left[\frac{(4aA-3\pi)}{3\pi} + \frac{gA}{L\Omega^2} \left(1 - \frac{A^2}{8} + \frac{A^4}{192} - \frac{A^6}{9216} + \frac{A^8}{737280} + \dots \right) \right] \cos \tau \\ &+ \left[\frac{12aA}{5\pi} - \frac{gA}{L\Omega^2} \left(\frac{A^2}{4} - \frac{A^4}{640} + \frac{A^6}{15360} - \frac{A^8}{1105920} + \dots \right) \right] \cos 3\tau \\ &+ \left[-\frac{20aA}{21\pi} + \frac{gA}{L\Omega^2} \left(\frac{A^4}{1920} - \frac{A^6}{46080} + \frac{A^8}{2580480} + \dots \right) \right] \cos 5\tau \\ &+ \left[\frac{28aA}{45\pi} - \frac{gA}{L\Omega^2} \left(\frac{A^6}{322560} - \frac{A^8}{10321920} + \dots \right) \right] \cos 7\tau + \left[-\frac{36aA}{77\pi} + \frac{gA}{L\Omega^2} \frac{A^8}{92897280} + \dots \right] \cos 9\tau + \dots \end{aligned}. \tag{29}$$

Taking into account Equations (8) and (29), we can choose the auxiliary functions in the form

$$\begin{aligned} A_1(\varphi_0(\tau), C_i) &= -(C_1 + 2C_2 \cos 2\tau + 2C_3 \cos 4\tau + 2C_4 \cos 6\tau) \\ A_2(\varphi_0(\tau), C_i) &= 0 \\ F(N[\varphi_0(\tau)]) &= \alpha \cos \tau + \beta \cos 3\tau + \gamma \cos 5\tau \end{aligned}, \tag{30}$$

where $C_1, C_2, C_3,$ and C_4 are unknown parameters and α, β, γ are obtained from Equation (29):

$$\begin{aligned} \alpha &= \frac{(4aA-3\pi)}{3\pi} + \frac{gA}{L\Omega^2} \left(1 - \frac{A^2}{8} + \frac{A^4}{192} - \frac{A^6}{9216} + \frac{A^8}{737280} \right) \\ \beta &= \frac{12aA}{5\pi} - \frac{gA}{L\Omega^2} \left(\frac{A^2}{32} - \frac{A^4}{384} + \frac{A^6}{15360} - \frac{A^8}{1105920} \right) \\ \gamma &= -\frac{20aA}{21\pi} + \frac{gA}{L\Omega^2} \left(\frac{A^4}{1920} - \frac{A^6}{46080} + \frac{A^8}{2580480} \right) \end{aligned}. \tag{31}$$

We also may choose the auxiliary functions A_1 and A_2 , and the function F as follows

$$\begin{aligned} A_1(\varphi_0(\tau), C_i) &= -(C_1 + 2C_2 \cos 3\tau + 2C_3 \cos 4\tau) \\ A_2(\varphi_0(\tau), C_i) &= C_4 \cos 5\tau \\ F(N[\varphi_0(\tau)]) &= \alpha \cos \tau + \beta \cos 3\tau \end{aligned}, \tag{32}$$

or

$$\begin{aligned} A_1(\varphi_0(\tau), C_i) &= -(C_1 + 2C_2 \cos 4\tau) \\ A_2(\varphi_0(\tau), C_i) &= C_3 \cos 3\tau + C_4 \cos 7\tau, \\ F(N[\varphi_0(\tau)]) &= \alpha \cos \tau + \gamma \cos 5\tau \end{aligned} \tag{33}$$

and so on.

Substituting Equation (30) into Equation (8), the result is

$$\begin{aligned} \varphi''_1 + \varphi_1 = & \frac{\alpha(C_1+C_2)+\beta(C_2+C_3)+\gamma(C_3+C_4)}{\Omega^2} \cos \tau \\ & + \frac{\alpha(C_2+C_3)+\beta(C_1+C_4)+\gamma C_2}{\Omega^2} \cos 3\tau + \frac{\alpha(C_3+C_4)+\beta C_2+\gamma C_1}{\Omega^2} \cos 5\tau \cdot \\ & + \frac{\alpha C_4+\beta C_3+\gamma C_2}{\Omega^2} \cos 9\tau + \frac{\gamma C_4}{\Omega^2} \cos 11\tau \end{aligned} \tag{34}$$

In order to avoid secular terms, the following condition should be imposed

$$\alpha(C_1 + C_2) + \beta(C_2 + C_3) + \gamma(C_3 + C_4) = 0. \tag{35}$$

From Equations (31) and (35) one retrieves

$$\Omega_{app}^2 = \frac{M}{\frac{3\pi-4aA}{3}(C_1 + C_2) - \frac{12aA(C_2+C_3)}{5} + \frac{20aA(C_3+C_4)}{21}}, \tag{36}$$

where

$$\begin{aligned} M = & \frac{\pi g A}{L} \left[(C_1 + C_2) \left(1 - \frac{A^2}{8} + \frac{A^4}{192} - \frac{A^6}{9216} + \frac{A^8}{737280} \right) \right. \\ & \left. - (C_2 + C_3) \left(\frac{A^2}{32} - \frac{A^4}{384} + \frac{A^6}{15360} - \frac{A^8}{1105920} \right) + (C_3 + C_4) \left(\frac{A^4}{1920} - \frac{A^6}{46080} + \frac{A^8}{2580480} \right) \right]. \end{aligned}$$

The solution (34) is given by

$$\begin{aligned} \varphi_1(\tau) = & \frac{\alpha(C_2+C_3)+\beta(C_1+C_4)+\gamma C_2}{8\Omega^2} (\cos \tau - \cos 3\tau) + \frac{\alpha(C_3+C_4)+\beta C_2+\gamma C_1}{24\Omega^2} (\cos \tau - \cos 5\tau) \\ & + \frac{\alpha C_4+\beta C_3+\gamma C_2}{48\Omega^2} (\cos \tau - \cos 7\tau) + \frac{\beta C_1+\gamma C_3}{80\Omega^2} (\cos \tau - \cos 9\tau) + \frac{\gamma C_4}{120\Omega^2} (\cos \tau - \cos 11\tau) \end{aligned} \tag{37}$$

From Equations (3), (23) and (37), and from the transformations $\tau = \Omega t$ and $\varphi = \theta A^{-1}$, one obtains the first-order approximate solution of Equation (16) as

$$\begin{aligned} \tilde{\theta}(t) = & A \cos \Omega t + \frac{A[\alpha(C_2+C_3)+\beta(C_1+C_4)+\gamma C_2]}{8\Omega^2} (\cos \Omega t - \cos 3\Omega t) \\ & + \frac{A[\alpha(C_3+C_4)+\beta C_2+\gamma C_1]}{24\Omega^2} (\cos \Omega t - \cos 5\Omega t) + \frac{A[\alpha C_4+\beta C_3+\gamma C_2]}{48\Omega^2} (\cos \Omega t - \cos 7\Omega t) , \\ & + \frac{A(\beta C_4+\gamma C_3)}{80\Omega^2} (\cos \Omega t - \cos 9\Omega t) + \frac{A\gamma C_4}{120\Omega^2} (\cos \Omega t - \cos 11\Omega t) \end{aligned} \tag{38}$$

where the coefficients α , β and γ are given in Equation (31) and Ω in Equation (36).

5. Results and Discussion

In order to emphasize the accuracy of our approach, we consider various sets of values for the parameters a , A , and L . We analyze the solution θ in 10 different cases and we develop comparisons between analytical and numerical integration results. Additionally, we represent a graphical comparison of the phase plane and a comparison between the frequencies Ω given by analytical developments (36) and numerical integration results, respectively. The calculation parameters were chosen as to reflect real cases, which could be encountered in practice.

5.1. Case 1

First, we consider $A = 0.1$, $a = 0.2$, $L = 0.6$, and $g = 9.8$. Using the proposed procedure, by minimizing the residual function, the optimal values of the convergence-control parameters C_i and the frequency (36) are

$$\begin{aligned} C_1 = & -0.02612929050874707; C_2 = 0.026479977489142312; \\ C_3 = & -0.0084357304447475517; C_4 = 0.0022006784301049727; \\ \Omega_{app} = & 4.056213309077129 \end{aligned}$$

The solution given by (38) can be written as follows:

$$\begin{aligned} \tilde{\theta}(t) = & 0.0998307842607 \cos \Omega t + 0.000186028849 \cos 3\Omega t - 0.000018350481 \cos 5\Omega t \\ & + 1.058064902746 \cdot 10^{-6} \cos 7\Omega t + 5.890466227595 \cdot 10^{-7} \cos 9\Omega t - 1.097402505723 \cdot 10^{-7} \cos 11\Omega t \end{aligned} \quad (39)$$

In Figures 2 and 3 is plotted the comparison between approximate solution (39) and numerical integration results, and the phase plane in this case, respectively.

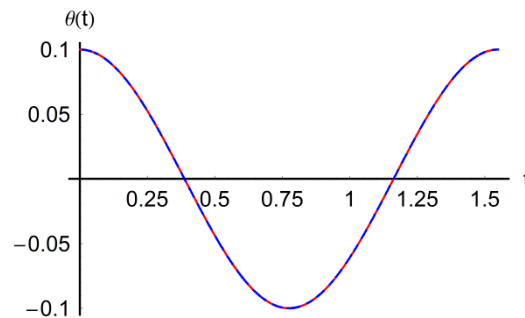


Figure 2. Comparison between the approximate solution (39) and numerical integration results for $A = 0.1, a = 0.2, L = 0.6$ — numerical — — approximate solution.

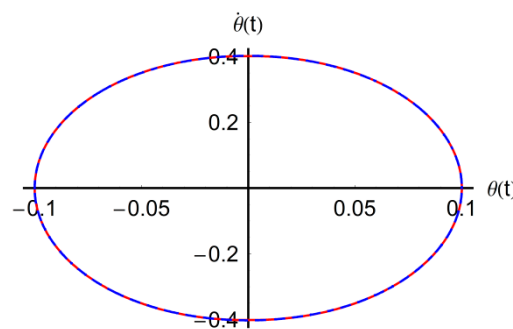


Figure 3. Phase plane for $A = 0.1, a = 0.2, L = 0.6$ — numerical — — approximate solution (39).

5.2. Case 2

For $A = 0.1, a = 0.4, L = 0.6$ we obtain

$$\begin{aligned} C_1 = & -0.06468511377430505; C_2 = 0.0663565183850488; \\ C_3 = & -0.024463908434927746; C_4 = 0.007981996714313724; \\ \Omega_{app} = & 4.0735339712576275 \end{aligned}$$

The solution given by (38) in this case can be written as follows:

$$\begin{aligned} \tilde{\theta}(t) = & 0.099649003276 \cos \Omega t + 0.000385656055 \cos 3\Omega t - 0.000036941545 \cos 5\Omega t \\ & - 2.769256927293 \cdot 10^{-7} \cos 7\Omega t + 3.355209133644 \cdot 10^{-6} \cos 9\Omega t - 7.960693115042 \cdot 10^{-7} \cos 11\Omega t \end{aligned} \quad (40)$$

The comparison between analytical solution (40) and numerical integration results is presented in Figures 4 and 5.

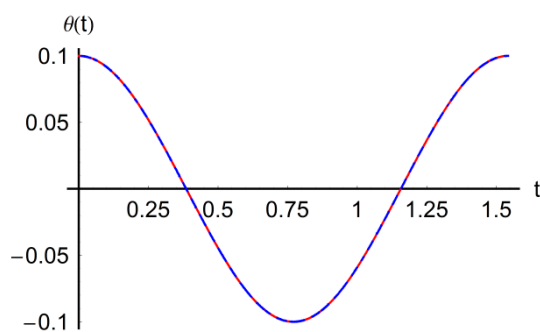


Figure 4. Comparison between the approximate solution (40) and numerical integration results for $A = 0.1, a = 0.4, L = 0.6$. — numerical - - - approximate solution.

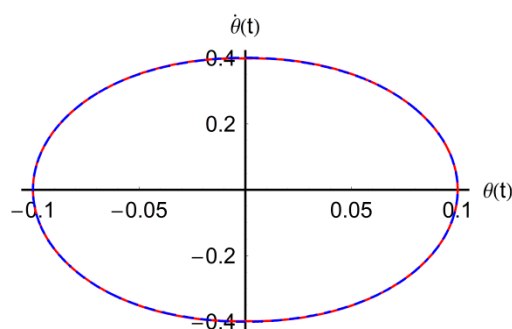


Figure 5. Phase plane for $A = 0.1, a = 0.4, L = 0.6$ — numerical - - - approximate solution (40).

5.3. Case 3

For $A = 0.1, a = 0.6, L = 0.6$ one can get

$$\begin{aligned}
 C_1 &= -0.1261219305\ 903601; C_2 = 0.1307654396\ 4819184; \\
 C_3 &= -0.0555663627\ 7721333; C_4 = 0.0210265079\ 04137733; \\
 \Omega_{app} &= 4.0917815705\ 13826
 \end{aligned}$$

$$\begin{aligned}
 \tilde{\theta}(t) &= 0.099462706082 \cos \Omega t + 0.000591204026 \cos 3\Omega t - 0.00005847843 \cos 5\Omega t \\
 &- 5.181840137296 \cdot 10^{-6} \cos 7\Omega t + 0.000011265133 \cos 9\Omega t - 3.145558315768 \cdot 10^{-6} \cos 11\Omega t
 \end{aligned} \tag{41}$$

Graphical comparisons between analytical and numerical results in this case are presented in Figures 6 and 7.

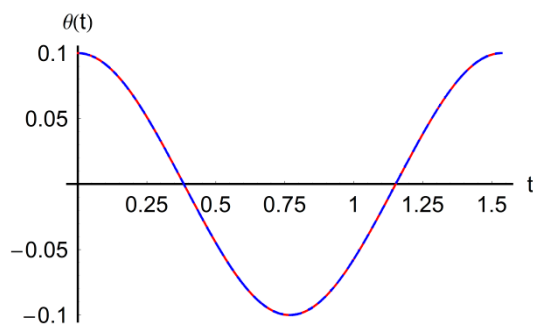


Figure 6. Comparison between the approximate solution (41) and numerical integration results for $A = 0.1, a = 0.6, L = 0.6$. — numerical - - - approximate solution.

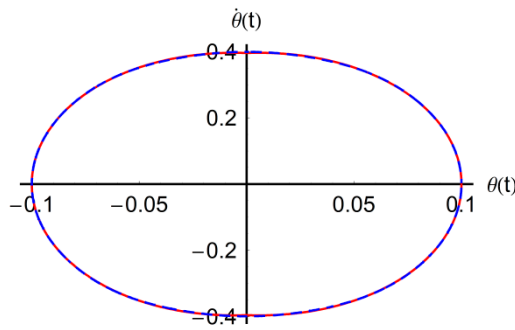


Figure 7. Phase plane for $A = 0.1, a = 0.6, L = 0.6$. — numerical - - - approximate solution (41).

5.4. Case 4

For $A = 0.2, a = 0.2, L = 0.6$, it holds that

$$C_1 = -0.0848611053\ 1011988; C_2 = 0.0871934689\ 9295516;$$

$$C_3 = -0.0365715419\ 8248718; C_4 = 0.0118502052\ 90770313;$$

$$\Omega_{app} = 4.0659463540\ 564085$$

$$\tilde{\theta}(t) = 0.1993020640806 \cos \Omega t + 0.000789686896 \cos 3\Omega t - 0.000099399722 \cos 5\Omega t - 3.173485847984 \cdot 10^{-8} \cos 7\Omega t + 0.000010044198 \cos 9\Omega t - 2.363718668036 \cdot 10^{-6} \cos 11\Omega t \quad (42)$$

Figures 8 and 9 emphasize the comparison of the analytical solution (42) with numerical integration results.

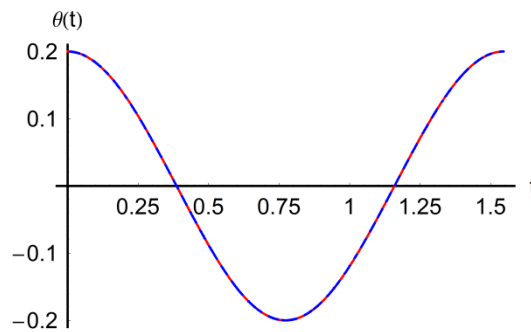


Figure 8. Comparison between the approximate solution (42) and numerical integration results for $A = 0.2, a = 0.2, L = 0.6$. — numerical - - - approximate solution.

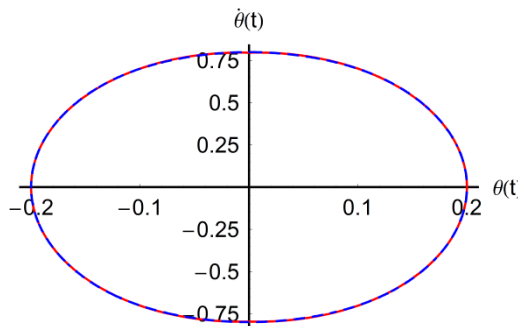


Figure 9. Phase plane for $A = 0.2, a = 0.2, L = 0.6$. — numerical - - - approximate solution (42).

5.5. Case 5

For $A = 0.2, a = 0.4, L = 0.6$, it holds that

$$C_1 = -0.0547821344 \ 6823842; C_2 = 0.0585371711 \ 5551574;$$

$$C_3 = -0.0046271807 \ 32353522; C_4 = 0.0202923559 \ 3370952;$$

$$\Omega_{app} = 4.1008614227 \ 769575$$

$$\tilde{\theta}(t) = 0.199076124329 \cos \Omega t + 0.000743701792 \cos 3\Omega t + 0.000180456966 \cos 5\Omega t$$

$$+ 8.131462054754 \cdot 10^{-6} \cos 7\Omega t - 3.192663647494 \cdot 10^{-7} \cos 9\Omega t - 8.095283729049 \cdot 10^{-6} \cos 11\Omega t \quad (43)$$

A comparison between the analytical solution (43) and corresponding numerical integration results is presented in Figures 10 and 11.

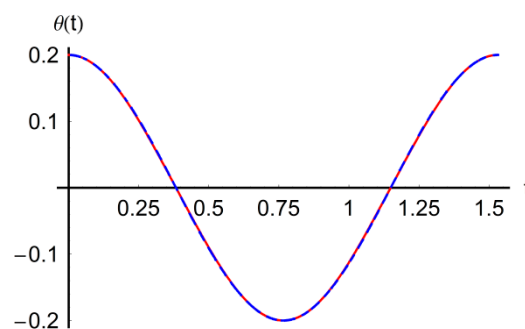


Figure 10. Comparison between the approximate solution (43) and numerical integration results for $A = 0.2, a = 0.4, L = 0.6$. — numerical — — approximate solution.

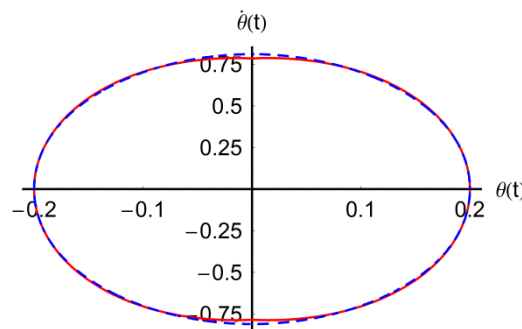


Figure 11. Phase plane for $A = 0.2, a = 0.4, L = 0.6$. — numerical — — approximate solution (43).

5.6. Case 6

For $A = 0.2, a = 0.6, L = 0.6$, we obtain

$$C_1 = 0.0300850261 \ 10128053; C_2 = -0.0355036855 \ 83418404;$$

$$C_3 = 0.0256650140 \ 4190474; C_4 = 0.0626909162 \ 6063286;$$

$$\Omega_{app} = 4.1374508035 \ 06345$$

$$\tilde{\theta}(t) = 0.199417 \cos \Omega t - 0.000080132 \cos 3\Omega t + 0.000496034 \cos 5\Omega t$$

$$+ 0.000241647 \cos 7\Omega t - 0.0000373673 \cos 9\Omega t - 0.0000375142 \cos 11\Omega t \quad (44)$$

In Figures 12 and 13 is plotted the comparison between approximate solution (44) and numerical integration results in this case.

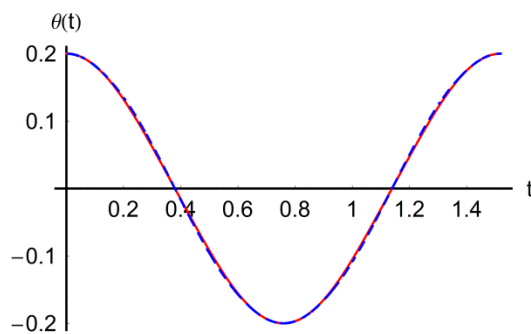


Figure 12. Comparison between the approximate solution (44) and numerical integration results for $A = 0.2, a = 0.6, L = 0.6$. — numerical — — approximate solution.

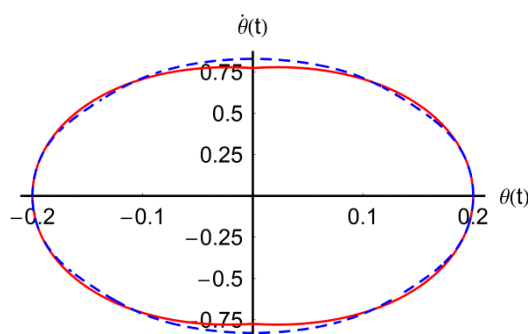


Figure 13. Phase plane for $A = 0.2, a = 0.6, L = 0.6$. — numerical — — approximate solution (44).

5.7. Case 7

In this case, for $A = 0.3, a = 0.2, L = 0.6$, yields

$$\begin{aligned}
 C_1 &= -0.1259868920\ 4928884; C_2 = 0.1319048242\ 7905972; \\
 C_3 &= -0.0532252516\ 8176718; C_4 = -0.0259636918\ 39690852; \\
 \Omega_{app} &= 4.0711925506\ 53585
 \end{aligned}$$

$$\begin{aligned}
 \tilde{\theta}(t) &= 0.298733 \cos \Omega t + 0.00129371 \cos 3\Omega t - 0.0000239776 \cos 5\Omega t \\
 &\quad - 0.0000223193 \cos 7\Omega t - 0.0000314489 \cos 9\Omega t - 0.0000116526 \cos 11\Omega t
 \end{aligned}
 \tag{45}$$

Graphical comparisons between analytical and numerical results are presented for this case in Figures 14 and 15.

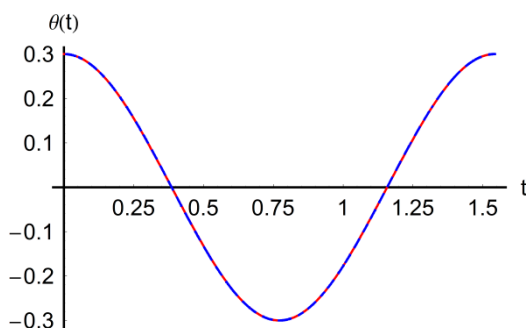


Figure 14. Comparison between the approximate solution (45) and numerical integration results for $A = 0.3, a = 0.2, L = 0.6$. — numerical — — approximate solution.

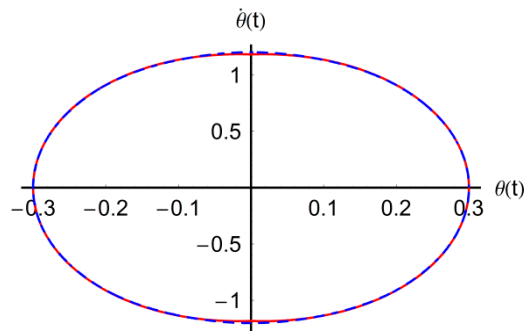


Figure 15. Phase plane for $A = 0.3, a = 0.2, L = 0.6$. — numerical — — — approximate solution (45).

5.8. Case 8

Considering $A = 0.3, a = 0.4, L = 0.6$, it follows that

$$\begin{aligned}
 C_1 &= 0.4719373259\ 762131; C_2 = -0.5063076905\ 748477; \\
 C_3 &= 0.3475612052\ 9541146; C_4 = -0.1153943661\ 8220579; \\
 \Omega_{app} &= 4.1252549407\ 44536
 \end{aligned}$$

$$\begin{aligned}
 \tilde{\theta}(t) &= 0.29784 \cos \Omega t + 0.001650441 \cos 3\Omega t + 0.000376774 \cos 5\Omega t \\
 &+ 0.000455463 \cos 7\Omega t - 0.000428294 \cos 9\Omega t + 0.000104476 \cos 11\Omega t
 \end{aligned}
 \tag{46}$$

Figures 16 and 17 emphasize the comparison of the analytical solution (46) with numerical integration results.

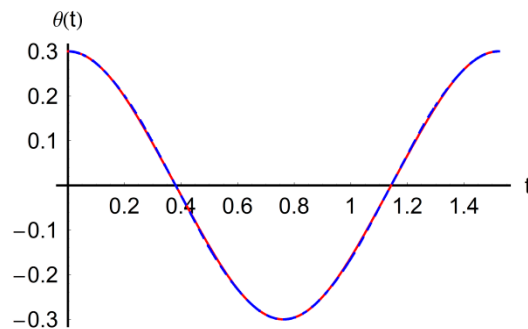


Figure 16. Comparison between the approximate solution (46) and numerical integration results for $A = 0.3, a = 0.4, L = 0.6$. — numerical — — — approximate solution.

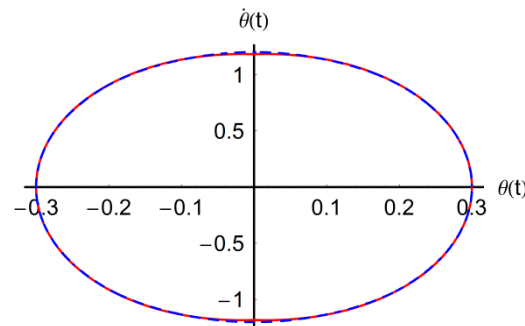


Figure 17. Phase plane for $A = 0.3, a = 0.4, L = 0.6$. — numerical — — — approximate solution (46).

5.9. Case 9

In this case, we consider $A = 0.3, a = 0.6, L = 0.6$, such that

$$\begin{aligned}
 C_1 &= 0.4150420146\ 527756; C_2 = -0.4611401944\ 978064; \\
 C_3 &= 0.3242095773\ 6633876; C_4 = -0.1212244132\ 9678995; \\
 \Omega_{app} &= 4.1807774631\ 05995
 \end{aligned}$$

$$\begin{aligned}
 \tilde{\theta}(t) &= 0.295522 \cos \Omega t + 0.00448745 \cos 3\Omega t - 0.000365785 \cos 5\Omega t \\
 &+ 0.000785393 \cos 7\Omega t - 0.000592619 \cos 9\Omega t + 0.000163216 \cos 11\Omega t
 \end{aligned}
 \tag{47}$$

Graphical comparisons between analytical and numerical results in this case are presented in Figures 18 and 19. Moreover Table 1 presents a comparison between the values of the frequency obtained in the above considered cases.

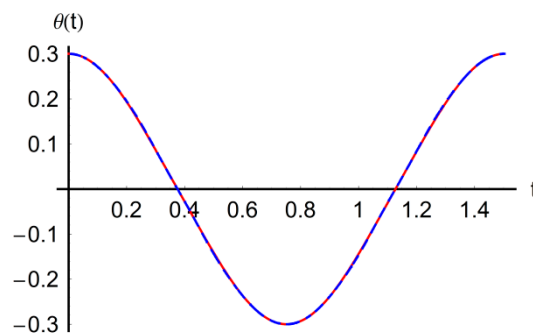


Figure 18. Comparison between the approximate solution (47) and numerical integration results for $A = 0.3, a = 0.6, L = 0.6$. — numerical — — approximate solution.

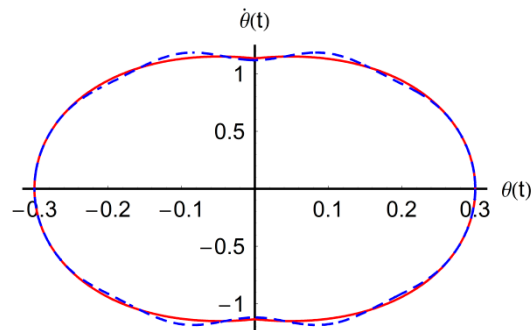


Figure 19. Phase plane for $A = 0.3, a = 0.6, L = 0.6$. — numerical — — approximate solution (47).

Table 1. Comparison between the numerical solution of the frequency and the approximate frequency (36).

Case No.	Ω_{num}	Ω_{app}
5.1	4.056165704763733	4.056213309077129
5.2	4.0735936668241015	4.0735339712576275
5.3	4.091213341156173	4.091781570513826
5.4	4.065980106247986	4.0659463540564085
5.5	4.10137202740024	4.1008614227769575
5.6	4.137539732217073	4.137450803506345
5.7	4.070864763571452	4.071192550653585
5.8	4.124733651749398	4.125254940744536
5.9	4.180380645932648	4.180777463105995

5.10. Case 10

The classical simple pendulum is obtained from Equation (16) in the case when no cylinder exists. Therefore, for $a = r/L = 0$ we obtain from (36) the approximate frequency

$$\Omega_{app}^2 = \frac{gA}{L} \left[1 - \frac{A^2}{8} + \frac{A^4}{192} - \frac{A^6}{9216} + \frac{A^8}{737280} - \frac{C_2+C_3}{C_1+C_2} \left(\frac{A^2}{32} - \frac{A^4}{384} + \frac{A^6}{15360} - \frac{A^8}{1105920} \right) + \frac{C_3+C_4}{C_1+C_2} \left(\frac{A^4}{1920} - \frac{A^6}{46080} + \frac{A^8}{2580480} \right) \right]. \tag{48}$$

The approximate solution for the simple pendulum is obtained from Equation (38) with the following coefficients given by Equation (31) for this particular case:

$$\begin{aligned} \alpha &= -\Omega^2 + \frac{gA}{L} \left(1 - \frac{A^2}{8} + \frac{A^4}{192} - \frac{A^6}{9216} + \frac{A^8}{737280} \right) \\ \beta &= -\frac{gA}{L} \left(\frac{A^2}{32} - \frac{A^4}{384} + \frac{A^6}{15360} - \frac{A^8}{1105920} \right) \\ \gamma &= \frac{gA}{L} \left(\frac{A^4}{1920} - \frac{A^6}{46080} + \frac{A^8}{2580480} \right) \end{aligned} \tag{49}$$

The optimal values of the control parameters and the approximate frequency in this case are, respectively

$$\begin{aligned} C_1 &= -0.0065766763\ 02841165; C_2 = 0.0065798727\ 04687396; \\ C_3 &= -0.0075433679\ 39537256; C_4 = 0.0013865133\ 762133064; \\ \Omega_{app} &= 3.9941012459\ 580407 \end{aligned}$$

$$\tilde{\theta}(t) = 0.4000837624301 \cos \Omega t - 0.000029363344 \cos 3\Omega t - 0.000061202307 \cos 5\Omega t + 6.789035888081 \cdot 10^{-6} \cos 7\Omega t + 1.421189152905 \cdot 10^{-8} \cos 9\Omega t - 2.506926263728 \cdot 10^{-11} \cos 11\Omega t \tag{50}$$

In Figure 20, we compared the results obtained through OAFM with numerical integration results for the particular care of simple pendulum for $A = 0.4, L = 0.6$, while in Figure 21 a comparison between the phase planes in this case is presented.

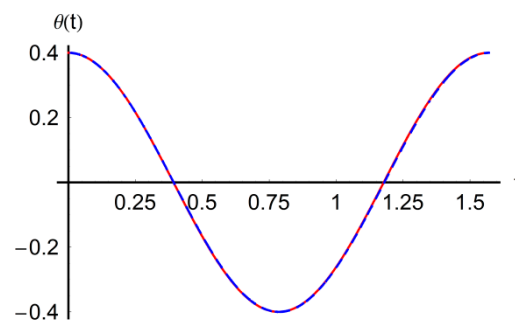


Figure 20. Comparison between the approximate solution (50) and numerical integration results for $A = 0.4, L = 0.6$. — numerical — — approximate solution.

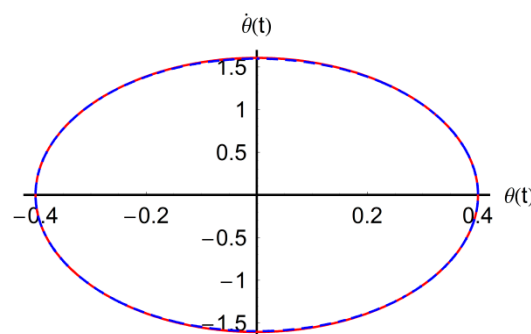


Figure 21. Phase plane for $A = 0.4, L = 0.6$. — numerical — — approximate solution (50).

Analyzing the comparison between the approximate and numerical integration results presented in Figures 2–21 for the cases 5.1–5.10, it can be observed that the results obtained by means of our procedure are almost identical with the results obtained using a numerical integration approach. Moreover, from Table 1 one can observe that the accuracy of the approximate frequency is remarkably good when compared to numerical results.

From Figures 2–19, it can be seen that the errors of the approximate solutions increase with respect to increasing values of the parameters a and A . Additionally, for the particular case of classical simple pendulum, the results obtained through our procedure are in very good agreement with numerical integration results. From the cases 5.4–5.6, and 5.7–5.8 respectively, we deduce that the frequency of the system is increased by increasing the radius of cylinders (parameter a). Additionally, from the cases 5.1, 5.4 and 5.7 it can be seen that the frequency of the system is increased by increasing the amplitude A . The same conclusion is obtained from the cases 5.2, 5.5 and 5.8 or 5.3, 5.6 and 5.9, respectively. The sources of nonlinear oscillations of the pendulum wrapping on two cylinders are given by the radius of cylinders (parameters a), the amplitude A and the length of pendulum.

6. Conclusions

In this paper we present an analytical and numerical solution for a pendulum wrapping on two cylinders, and also the corresponding frequencies using both a new analytical approach, namely the Optimal Auxiliary Functions Method (OAFM), and a numerical integration approach. To validate the approximate solutions obtained by means of OAFM it is necessary to present the time response for different cases.

The proposed analytical approach, OAFM, accelerates the convergence of the approximate solutions of nonlinear pendulum wrapping on two cylinders and lead to very accurate values of frequencies. The construction of the first iteration is totally different from any other known approach, mainly concerning the presence of the optimal auxiliary functions dependent on the convergence-control parameters. It should be emphasized that in the construction given by Equation (8), especially for very complicated equations of type (1), it is not needed for the presence of the entire nonlinear function $N[u_0(x)]$ and as a consequence, a considerable simplification is observed for the treatment of the first approximation $u_1(x, C_i)$. On the other hand, within Equation (8), the auxiliary functions A_1 and A_2 compensate the presence of nonlinear function $N[u_0(x)]$.

The initially unknown parameters C_i whose optimal values are determined using rigorous criterion, ensure a rapid convergence of the approximate analytical solutions since accurate results are obtained after the first iteration.

The great advantage of the OAFM is the possibility to optimally control and adjust the convergence of the solutions with the help of the auxiliary functions A_1 and A_2 .

The resulting analytical solutions proved to be in very good agreement with numerical integration ones and this proves the validity of the proposed method, emphasizing that this procedure is very efficient in practice.

The OAFM could be easily extended to faulted rotary systems, such as cracked or rubbing rotors [31,32], which will be the authors' future research direction. Moreover, in order to test the capabilities of the proposed approach, another future research will be directed to provide a comparison between OAFM and harmonic balance method [33] in solving nonlinear dynamic problems.

Author Contributions: Conceptualization, V.M. and N.H.; formal analysis, V.M.; investigation, V.M. and N.H.; methodology, V.M. and N.H.; validation, N.H.; writing—original draft, V.M. and N.H. All authors have read and agreed to the published version of the manuscript.

Funding: This research received no external funding.

Conflicts of Interest: The authors declare no conflict of interest.

References

1. Stillman, D. *Galileo at Work: His Scientific Biography*; Courier Corporation: North Chelmsford, MA, USA; Dover Corporation: Downers Grove, IL, USA, 2003.
2. Matthews, R.M. *Time for Science Education: How Teaching the History and Philosophy of Pendulum Motion Can Contribute to Science Literacy*; Springer: New York, NY, USA, 2000.
3. Aczel, A. Leon Foucault: His life, times and achievements. In *The Pendulum: Scientific, Historical, Educational and Philosophical Perspectives*; Matthews, M.R., Gauld, C.F., Stinner, A., Eds.; Springer: Berlin/Heidelberg, Germany, 2005; pp. 171–184.
4. Marrison, W. The evolution of the quartz crystal clock. *Bell Syst. Tech. J.* **1948**, *27*, 510–588. [[CrossRef](#)]
5. Audoin, C.; Guinot, B.; Lyle, S. *The Measurement of Time, Frequency and the Atomic Clock*; Cambridge University Press: Cambridge, UK, 2001.
6. Willis, M. *Time and Timekeepers*; MacMillan: New York, NY, USA, 1945.
7. Airy, G.B. On the disturbances of pendulum and balances and on the theory of escapements. *Trans. Camb. Philos. Soc.* **1830**, *III*, 105–128.
8. Lenzen, V.F.; Multauf, R.P. *Development of Gravity Pendulums in the 19-th Century*; United States National Museum Bulletin: Washington, DC, USA, 1964; Volume 240.
9. Hamouda, M.N.H.; Pierce, G.A. Helicopter vibration suppression using simple pendulum absorbers on the rotor blade. *J. Am. Helicopter Soc.* **1984**, *23*, 19–29. [[CrossRef](#)]
10. Nelson, R.A.; Olsson, M.G. The pendulum-Rich physics from a simple system. *Am. J. Phys.* **1986**, *54*, 112–121. [[CrossRef](#)]
11. Ge, Z.M.; Ku, F.N. Subharmonic Melnikov functions for strongly odd nonlinear oscillators with large perturbations. *J. Sound Vib.* **2000**, *236*, 554–560. [[CrossRef](#)]
12. Nester, T.M.; Schnitz, P.M.; Haddow, A.G.; Shaw, S.W. Experimental Observations of Centrifugal Pendulum Vibration Absorber. In Proceedings of the 10th International Symposium on Transport Phenomena and Dynamics of Rotating Machinery (ISROMAC-10), Honolulu, HI, USA, 7 March 2004.
13. Bendersky, S.; Sandler, B. Investigation of a spatial double pendulum: An engineering approach. *Discret. Dyn. Nat. Soc.* **2006**, *2006*, 25193. [[CrossRef](#)]
14. Horton, B.; Sieber, J.; Thompson, J.M.T.; Wiercigroch, M. Dynamics of the nearly parametric pendulum. *Int. J. Nonlinear Mech.* **2011**, *46*, 436–442. [[CrossRef](#)]
15. Warminski, J.; Kecik, K. Autoparametric vibrations of a nonlinear system with pendulum. *Math. Probl. Eng.* **2006**, *2006*, 80705. [[CrossRef](#)]
16. Kecik, K.; Warminski, J. Dynamics of an autoparametric pendulum-like system with a nonlinear semiactive suspension. *Math. Probl. Eng.* **2011**, *2011*, 451047. [[CrossRef](#)]
17. Rafat, M.Z.; Wheatland, M.S.; Bedding, T.R. Dynamics of a double pendulum with distributed mass. *Am. J. Phys.* **2009**, *77*, 216–222. [[CrossRef](#)]
18. Turkilazoglu, M. Accurate analytic approximation to the nonlinear pendulum problem. *Phys. Scr.* **2011**, *84*, 015005. [[CrossRef](#)]
19. Awrejcewicz, J. *Classical Mechanics: Dynamics. Advances in Mechanics and Mathematics*; Springer: Berlin/Heidelberg, Germany, 2012.
20. Ludwicki, M.; Awrejcewicz, J.; Kudra, G. Spatial double physical pendulum with axial excitation—Computer simulation and experimental set-up. *Int. J. Dyn. Control.* **2015**, *3*, 1–8. [[CrossRef](#)]
21. Starosta, R.; Sypniewska-Kaminska, G.; Awrejcewicz, J. Parametric and external resonances in kinematically and externally excited nonlinear spring pendulum. *Int. J. Bifurc. Chaos* **2011**, *21*, 3013–3021. [[CrossRef](#)]
22. Bayat, M.; Pakar, I.; Bayat, M. Application of He's energy balance method for pendulum attached to rolling wheels that are restrained by a spring. *Int. J. Phys. Sci.* **2012**, *7*, 913–921.
23. Mazaheri, H.; Hosseinzadeh, A.; Ahmadian, M.T. Nonlinear oscillation analysis of a pendulum wrapping on a cylinder. *Sci. Iran. B* **2012**, *119*, 335–340. [[CrossRef](#)]
24. Boubaker, O. The inverted pendulum benchmark in nonlinear control theory: A survey. *Int. J. Adv. Robot. Syst.* **2013**, *10*, 1–5. [[CrossRef](#)]
25. Alevras, P.; Yurchenko, D.; Naess, A. Stochastic synchronization of rotating parametric pendulums. *Meccanica* **2014**, *49*, 1945–1951. [[CrossRef](#)]

26. Jallouli, A.; Kacem, N.; Bouhaddi, N. Stabilization of solitons in coupled nonlinear pendulums with simultaneous external and parametric excitation. *Commun. Nonlinear Sci. Numer. Simul.* **2017**, *42*, 1–11. [[CrossRef](#)]
27. Herisanu, N.; Marinca, V. An efficient analytical approach to investigate the dynamics of a misaligned multirotor system. *Mathematics* **2020**, *8*, 1083. [[CrossRef](#)]
28. Herisanu, N.; Marinca, V.; Madescu, G.; Dragan, F. Dynamic response of a permanent magnet synchronous generator to a wind gust. *Energies* **2019**, *12*, 915. [[CrossRef](#)]
29. Marinca, V.; Herisanu, N. An optimal iteration method with application to the Thomas-Fermi equation. *Cent. Eur. J. Phys.* **2011**, *9*, 891–895. [[CrossRef](#)]
30. Marinca, V.; Herisanu, N. Explicit and exact solutions to cubic Duffing and double-well Duffing equations. *Math. Comput. Model.* **2011**, *53*, 604–609. [[CrossRef](#)]
31. Fu, C.; Xu, Y.; Yang, Y.; Lu, K.; Gu, F.; Ball, A. Dynamics analysis of a hollow-shaft rotor system with an open crack under model uncertainties. *Commun. Nonlinear Sci. Numer. Simul.* **2020**, *83*, 105102. [[CrossRef](#)]
32. Fu, C.; Zhen, D.; Yang, Y.; Gu, F.; Ball, A. Effects of bounded uncertainties on the dynamic characteristics of an overhung rotor system with rubbing fault. *Energies* **2019**, *12*, 4365. [[CrossRef](#)]
33. Li, H.; Chen, Y.; Hou, L.; Zhang, Z. Periodic response analysis of a misaligned rotor system by harmonic balance method with alternating frequency/time domain technique. *Sci. China Technol. Sci.* **2016**, *59*, 1717–1729. [[CrossRef](#)]



© 2020 by the authors. Licensee MDPI, Basel, Switzerland. This article is an open access article distributed under the terms and conditions of the Creative Commons Attribution (CC BY) license (<http://creativecommons.org/licenses/by/4.0/>).